

Diffusion-weighted and perfusion MRI demonstrates parenchymal changes in complex partial status epilepticus

Kristina Szabo,¹ Annkathrin Poepel,² Bernd Pohlmann-Eden,³ Jochen Hirsch,¹ Tobias Back,¹ Oliver Sedlaczek,¹ Michael Hennerici¹ and Achim Gass¹

¹Department of Neurology, Universitätsklinikum Mannheim, University of Heidelberg, Mannheim, ²Department of Epileptology, University of Bonn Medical Center, Bonn and ³Epilepsy Centre Bethel, Bielefeld, Germany

Correspondence to: Achim Gass, MD, MR Research Neurology, Department of Neurology, Universitätsklinikum Mannheim, Theodor-Kutzer-Ufer, 68137 Mannheim, Germany
E-mail: gass@neuro.ma.uni-heidelberg.de

Summary

Diffusion-weighted MRI (DWI) and perfusion MRI (PI) have been mainly applied in acute stroke, but may provide information in the peri-ictal phase in epilepsy patients. Both transient reductions of brain water diffusion, namely a low apparent diffusion coefficient (ADC), and signs of hyperperfusion have been reported in experimental and human epilepsy case studies. We studied 10 patients with complex partial status epilepticus (CPSE) with serial MRI including DWI and PI. All patients showed regional hyperintensity on DWI, and a reduction of the ADC in (i) the hippocampal formation and the pulvinar region of the thalamus (six out of 10 patients), (ii) the pulvinar and cortical regions (two out of 10), (iii) the hippocampal formation only (one out of 10), and (iv) the hippocampal

formation, the pulvinar and the cortex (one out of 10). In all patients a close spatial correlation of focal hyperperfusion with areas of ADC/DWI change was present. In two patients hyperperfusion was confirmed in additional SPECT (single photon emission computed tomography) studies. All patients received follow-up MRI examinations showing partial or complete resolution of diffusion and perfusion abnormalities depending on the length of the follow-up interval. The clinical course, EEG and SPECT results all indicate that MRI detected changes related to prolonged epileptic activity. Combined PI and DWI can visualize haemodynamic and tissue changes after CPSE in the hippocampus, thalamus and affected cortical regions.

Keywords: magnetic resonance imaging; diffusion; perfusion; epilepsy

Abbreviations: ADC = apparent diffusion coefficient; CBF = cerebral blood flow; CBV = cerebral blood volume; CPSE = complex partial status epilepticus; DWI = diffusion-weighted MRI; MCA = middle cerebral artery; MTT = mean transit time; MRA = magnetic resonance angiography; PCA = posterior cerebral artery; PI = perfusion MRI; ROI = region of interest; SPECT = single photon emission computed tomography; TTP = time to peak

Received September 26, 2004. Revised December 23, 2004. Accepted January 25, 2005. Advance Access publication March 2, 2005

Introduction

Haemodynamic changes associated with ictal activity were described intraoperatively by Penfield (Penfield, 1933) and were noted as hypervascular patterns in angiographic studies (Stone *et al.*, 1986; Lee and Goldberg, 1977). In focal epilepsy, areas of hyperperfusion have been identified with ictal ^{99m}Tc-HMPAO single photon emission computed tomography (SPECT) (Markand *et al.*, 1997). With MRI, it has been possible to demonstrate similar changes in several case studies. Using perfusion MRI (PI), Warach *et al.* demonstrated ictal

hyperperfusion in a patient with focal epilepsy (Warach *et al.*, 1994). Focal haemodynamic alterations related to focal ictal activity have also been reported by Jackson *et al.* and Detre *et al.* employing the blood oxygenation level-dependent (BOLD) MRI method (Jackson *et al.*, 1994; Detre *et al.*, 1995).

Apart from MRI techniques that can visualize haemodynamic changes, a current focus of interest has been diffusion-weighted MRI (DWI). Transient reductions of the apparent diffusion coefficient (ADC) have been detected with

Table 1 Patient profiles

Patient	Age, sex	Primary cerebral pathology/ previous diagnosed epilepsy	Seizure profile			Timing of MRI	
			Type/signs	Clinical duration	EEG	Initial	Follow-up
1	59, M	Chronic residual small cortical haemorrhage after cortical vein thrombosis/yes (Fig. 4)	CPSE; mild CI	4 days	Right parietotemporal rhythmic focal slowing (seizure pattern), PLEDs	3.5 h	Day 2, day 13, months 1, 10
2	66, F	Chronic residual cortical haemorrhage in isolated cerebral vasculitis/yes (Fig. 2A)	CPSE; mild CI	2 days	Right temporo-occipital, rhythmic SW, partially generalized	8.5 h	Day 2, day 7, months 4, 9
3	38, F	Hippocampal sclerosis in temporal lobe epilepsy/yes (Fig. 1A)	TC, CPSE; mild CI	2 days	Left temporo-occipital rhythmic delta, mixed with SW	6 h	Day 7
4	73, M	Previous ICA occlusion with chronic stroke and hypoperfusion of MCA territory/no (Figs 1B, 2B)	CPSE; mild CI	3 days	Left temporal rhythmic SW	12 h	Day 14
5	68, M	Previous frontal head trauma/yes	CPSE; mild CI	4 days	Left temporal rhythmic SW	12 h	Lost to follow-up
6	27, F	Chronic MCA stroke/no (Figs 1C, 2C)	CPSE; mild CI	3 days	Left temporal rhythmic SW	3 h	Day 2 (day 4 [†])
7	76, F	Chronic and acute MCA stroke/no (Fig. 1D)	CPSE; mild CI	6 days	Left temporal rhythmic SW	24 h	Month 3
8	56, F	Chronic MCA and PCA stroke/no	CPSE; mild CI	4 day	Left temporal focal slowing (postictal)	6 h	Day 7
9	78, M	Cerebral microangiopathy/no (Fig. 1E)	CPSE; severe CI	3 days	Left temporal focal slowing (postictal)	5 h	Day 7, month 5
10	55, M	Glioblastoma multiforme/no (Figs 2D, 3)	CPSE; mild CI	3 h	Left temporo-occipital focal slowing (postictal)	3.5 h	Day 7

ICA = internal carotid artery; MCA = middle cerebral artery; PCA = posterior cerebral artery; CPSE = complex partial status epilepticus; TC = tonic-clonic seizures; CI = cognitive impairment; PLEDs = periodic lateralized epileptiform discharge; SW = sharp waves. Timing of MRI: Initial = timing from seizure onset to MRI.

† = deceased.

DWI in experimental focal ischaemia with peri-infarct depolarizations, and in models of spreading depression and models of epilepsy (Gyngell *et al.*, 1994; Zhong *et al.*, 1995; de Crespiigny *et al.*, 1998). Fabene and colleagues found DWI and T2-weighted changes throughout the cerebral cortex, hippocampus, amygdala and medial thalamus in rat brains after 4 h of status epilepticus (Fabene *et al.*, 2003). Several case studies have demonstrated reduced ADCs in patients with focal status epilepticus (Wiesmann *et al.*, 1997; Diehl *et al.*, 1999; Lansberg *et al.*, 1999; Kim *et al.*, 2001). Another recent study reported transient ADC changes immediately after single seizures (Hufnagel *et al.*, 2003). Despite evidence for the relationship between ictal activity and altered haemodynamic state, there are no systematic studies on the combined use of DWI and PI in epilepsy, although this methodology is commonly used to investigate acute stroke patients.

We investigated the combined use of DWI and PI in a series of 10 patients presenting with complex partial status epilepticus (CPSE) who had acute and follow-up MRI.

Subjects and methods

Subjects

We examined 10 consecutive patients (five men, five women, mean age 59.6 years, range 27–78 years) presenting with complex partial

status epilepticus (CPSE) using MRI in the peri-ictal phase and on follow-up. All patients were seen in the emergency room from 1998 to 2002 in confusional states that were eventually diagnosed as CPSE (Shneker and Fountain, 2003). One patient had a previously confirmed diagnosis of temporal lobe epilepsy as the cause of ictal activity; the remaining nine patients had acute symptomatic seizures due to different primary pathologies, and in four the diagnosis of symptomatic epilepsy had been established previously. The clinical and EEG data of the patients are summarized in Table 1. Two patients additionally underwent SPECT within 24 h after the initial MRI. The study was approved by the local ethics committee and for all patients the responsible relative gave informed consent in writing.

Data acquisition

MRI was performed with a 1.5 T MRI system (Siemens, Erlangen, Germany) according to the following protocol: (i) separate transverse, coronal and sagittal localizing sequences followed by transverse oblique contiguous images (slice thickness 5 mm) aligned with the inferior borders of the corpus callosum (sequences 2–7); (ii) proton density (PD)- and T2-weighted [turbo spin echo, repetition time (TR) 2620 ms, echo time (TE) 14 ms/85 ms, field of view (FOV) 180 × 240 mm², matrix size 192 × 256]; (iii) T1-weighted Spin echo (SE) (TR 530 ms, TE 12 ms, FOV 180 × 240 mm², matrix size 192 × 256); (iv) diffusion weighted echo planar spin echo (DW EP-SE) (TR 4000 ms, TE 110 ms, $b = 0/1000$ s/mm², FOV 240 mm², matrix size 128 × 128, sequential application of three separate

diffusion-sensitizing gradients in perpendicular directions) (further transverse DWI sequences aligned with the hippocampal formation were also performed); (v) FLAIR (fluid attenuation inversion recovery) (TR 9000 ms, TE 105 ms, inversion time (TI) 2340 ms, FOV $180 \times 240 \text{ mm}^2$, matrix size 192×256); (vi) three-dimensional time-of-flight magnetic resonance angiography (MRA) sequence (flip angle 20° , FOV $180 \times 240 \text{ mm}^2$, matrix size 165×512 , slice thickness 2 mm); (vii) perfusion free induction decay echo planar (FID-EP) sequence following the first pass of a contrast bolus through the brain (TR 2000 ms, TE 65 ms, flip angle 90° , 13 slices, 40 acquisitions, 1 : 20 min, FOV 240 mm^2 , matrix size 128×128). Contrast agent was injected with a flow rate of 4 ml/s through a large gauge venous cannula at the antecubital vein.

Data processing and qualitative/quantitative analysis

Structural MRI data (T1-weighted, PD- and T2-weighted, FLAIR) were analysed for pre-existing chronic abnormalities. DWI, PI and MRA were analysed for additional signal abnormalities as follows.

Changes on DWI were first analysed visually for hyperintense lesions. In addition to DWI, ADC maps were calculated on a pixel-by-pixel basis using a linear least-squares fit. The ADC was determined with manually defined regions of interest (ROI, size $0.2\text{--}0.5 \text{ cm}^2$), which were positioned in the regions of most pronounced signal change on DWI ($b = 1000 \text{ s/mm}^2$) (Fig. 3, ROI in green). ADC values were compared with the those of the contralateral normal hemisphere, the values of which correlated with previously obtained ADC values in normal controls (for stroke studies) (Gass *et al.*, 1999).

From the PI data set parameter maps, time to peak (TTP), mean transit time (MTT), relative cerebral blood volume (CBV) and relative cerebral blood flow (CBF) were calculated using the non-parametric singular-value decomposition method described by Ostergaard and colleagues (Ostergaard *et al.*, 1996; Yamada *et al.*, 2002). This method involves deconvolution of the tissue concentration–time curve on a pixel-by-pixel basis with an arterial input function. Maps of CBF and CBV are determined from the peak height and the area under the deconvolved curve, respectively. All perfusion maps were analysed for the presence and location of signal changes indicating hyperperfusion (reduced TTP, reduced MTT, increased CBV, increased CBF) or hypoperfusion (prolonged TTP, prolonged MTT, reduced or normal CBV, reduced CBF).

Results

Clinical data and conventional MRI

All patients presented with acute confusional states classified as mild or severe cognitive impairment, as proposed by Shneker and colleagues. Clinical symptoms were considered mild if the patient was awake but confused and severe if the patient was obtunded or comatose (Shneker and Fountain, 2003). In addition to mild cognitive impairment, patient 1 developed clonic left-sided seizure activity during the last sequence of the MRI examination, which stopped immediately after administration of 10 mg diazepam. Except cases 8 and 9, who had CPSE of long duration, there was close timing between EEG and MRI (mean 1.8 h delay between EEG and MRI). Focal seizure activity on EEG was found in seven out of 10 patients, while in three cases postictal EEG showed

focal slowing. Structural abnormalities on conventional MRI caused by various pathologies were found in all patients. Two patients had chronic parenchymal alterations after previous haemorrhages close to the cortex (patients 1 and 2). In patient 1 haemorrhage had occurred due to venous thrombosis. In patient 2 previous haemorrhage was due to histopathologically proven isolated cerebral vasculitis. Patient 3 had right hippocampal sclerosis diagnosed earlier in the context of longstanding temporal lobe epilepsy. One patient had a traumatic lesion in the left frontal cortex acquired in a car accident 1 year earlier (patient 5). Three patients had chronic ischaemic lesions which had occurred at least 8 months earlier: the first patient (patient 4) had haemodynamic infarction due to occlusion of the internal carotid artery with persistent hypoperfusion of the affected hemisphere, the second patient (patient 6) had chronic middle cerebral artery (MCA) stroke of embolic origin, and the third a chronic MCA and posterior cerebral artery (PCA) stroke (patient 8). One patient had both an acute and a chronic MCA territory lesion in the parietal region due to a MCA stenosis (patient 7). One patient showed subcortical white matter lesions and signs of cortical atrophy (patient 9). Patient 10 had a right parietal solitary mass lesion, histologically diagnosed subsequently as glioblastoma multiforme. Under anti-epileptic drug therapy clinical findings and EEG abnormalities improved and eventually resolved in all patients.

Ictal/peri-ictal lesions on diffusion-weighted, T2-weighted and perfusion images

In all patients, analysis of MRIs revealed slight focal swelling accompanied by hyperintensity on T2-weighted images and increased signal intensity on DWI (Table 2). In nine out of 10 patients lateralization and localization of EEG pathology corresponded with the acute DWI pathology. In all patients, ROI analysis of ADC values taken from regions with most pronounced signal change were reduced by 11–37% (see Table 2 for details).

DWI and ADC signal change was limited to the hippocampal formation in one case (patient 8). Six patients showed acute lesions in the hippocampus and in the ipsilateral posterior part of the thalamus, the region of the pulvinar nuclei (patients 3, 4, 5, 6, 7 and 9), while two patients had signal alterations in cortical regions, affecting mainly cortical tissue and some underlying white matter, and in the ipsilateral pulvinar (patients 1 and 10). Finally, in one patient the cortex, hippocampus and pulvinar were involved and showed signal alterations (patient 2). Figures 1 and 2 show the consistency of acute hippocampal and thalamic involvement on DWI images.

All patients showed subtle but obvious signs of hyperperfusion on TTP, MTT and CBV maps, which were confirmed by additional SPECT studies in two patients (patients 1 and 2; Fig. 4). The hyperperfused regions matched the regions of DWI signal abnormalities in all cases, but were slightly larger

Table 2 MRI findings

Patient	Acute ictal/peri-ictal signal abnormality		Follow-up	
	DWI/T2/PWI/MRA	Location and size of DWI hyperintensity	DWI/T2/PWI follow-up	Conventional MRI findings
1	DWI ↑; ADC ↓ (-35%); T2 →; PWI ↑ (+SPECT)	Right parieto-occipital cortex and right pulvinar; 12 ml	Complete resolution of PWI (day 2), DWI (day 13), T2 (month 1) abnormalities	Previous small haemorrhage after cortical vein thrombosis
2	DWI ↑, ADC ↓ (-37%); T2 ↑; PWI ↑ (+SPECT)	Right hippocampal formation, right pulvinar and right parieto-occipital cortex; 5.2 ml	Complete resolution of DWI/T2/PWI abnormalities (month 4)	Chronic right occipital intracranial haemorrhage in cerebral vasculitis
3	DWI ↑, ADC ↓ (-28%); T2 ↑; PWI ↑	Right hippocampal formation and right pulvinar; 1.5 ml	Resolution of PWI, partial resolution of DWI/T2 signal change (day 7)	Right hippocampal sclerosis
4	DWI ↑; ADC ↓ (-22%); T2 ↑; PWI ↑, PCA ↑	Left hippocampal formation and left pulvinar; 1.9 ml	Complete resolution of DWI/T2/PWI abnormalities (day 14)	Chronic white matter lesions; occlusion of left ICA with hypoperfusion of left MCA territory
5	DWI ↑; ADC ↓ (-11%); T2 ↑; PWI ↑	Left hippocampal formation and left pulvinar; 1.6 ml	Lost to follow-up	Left frontopolar post-traumatic lesion
6	DWI ↑, ADC ↓ (-25%); T2 ↑; PWI ↑, PCA ↑	Left hippocampal formation and left pulvinar; 1.5 ml	Resolution of PWI, partial resolution of DWI/T2 signal change (day 2)	Chronic left temporoparietal MCA stroke; MCA stenosis and hypoperfusion
7	DWI ↑, ADC ↓ (-25%); T2 ↑; PWI ↑	Left hippocampal formation and left pulvinar; 1.9 ml	Complete resolution of DWI/T2/PWI abnormalities (month 3)	Acute and chronic left temporoparietal MCA stroke; MCA stenosis and hypoperfusion
8	DWI ↑, ADC ↓ (-13%); T2 ↑; PWI ↑, PCA ↑	Left hippocampal formation; 1.4 ml	Resolution of PWI, partial resolution of DWI/T2 signal change (day 7)	Chronic right MCA and PCA stroke
9	DWI ↑, ADC ↓ (-22%); T2 ↑; PWI ↑, PCA ↑	Left hippocampal formation and left pulvinar; 1.7 ml	Complete resolution of DWI/T2/PWI abnormalities (month 5)	Cortical atrophy, chronic white matter lesions
10	DWI ↑; ADC ↓ (-34%); T2 →; PWI ↑	Extensive right temporal and parietal cortical involvement; right pulvinar; 10 ml	Resolution of PWI, partial resolution of DWI/T2 signal change (day 7)	Right parietal glioblastoma

DWI ↑ = hyperintensity; ADC ↓ = reduction (%); PWI ↑ = signs of hyperperfusion; PCA ↑ = increased flow signal in the PCA; MCA = middle cerebral artery; PCA = posterior cerebral artery; ICA = internal carotid artery.

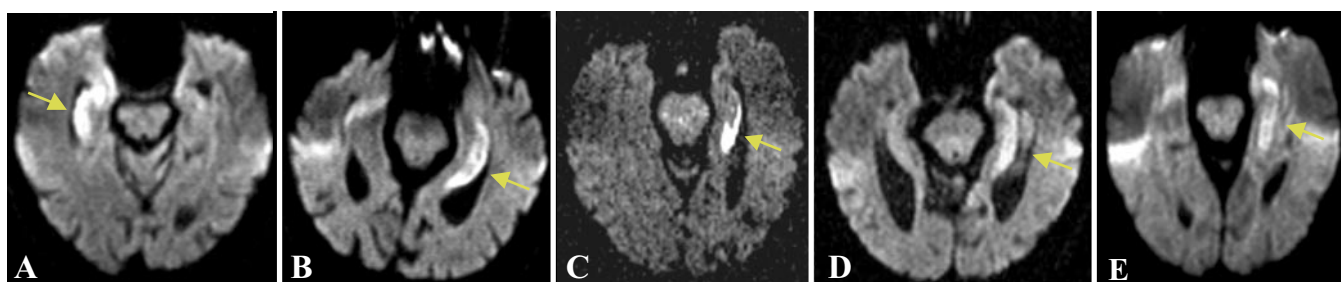


Fig. 1 Diffusion-weighted MRI demonstrating involvement of the hippocampus in patients 3, 4, 6, 7 and 9. High-intensity signal abnormality is noted in the right (A) and left (B–E; arrows) hippocampus. Hyperintense susceptibility artefacts can occasionally be seen in the area of the temporal bone.

in size. In four patients (patients 4, 6, 8 and 9) with hyperperfusion of the hippocampal formation, MRA also showed increased flow signal in the ipsilateral PCA compared with the contralateral side, indicating the enhanced blood flow. In patients 4, 6 and 7, all with chronic hypoperfusion in the left MCA territory, local hyperperfusion was identified in the adjacent PCA territory supplying the left hippocampal formation, the region of DWI abnormalities.

Follow-up MRI

All but one patient were studied subsequently with one to four follow-up MRI examinations (for details see Table 1). PI signal change did not persist, but normalized, showing identical signal characteristics as the contralateral normal vascular territory/hemisphere on PI maps or MRA, on the first follow-up in nine out of nine patients. Slight DWI hyperintensity was still noted in patients 3, 6, 8 and 10, who had follow-up MRI

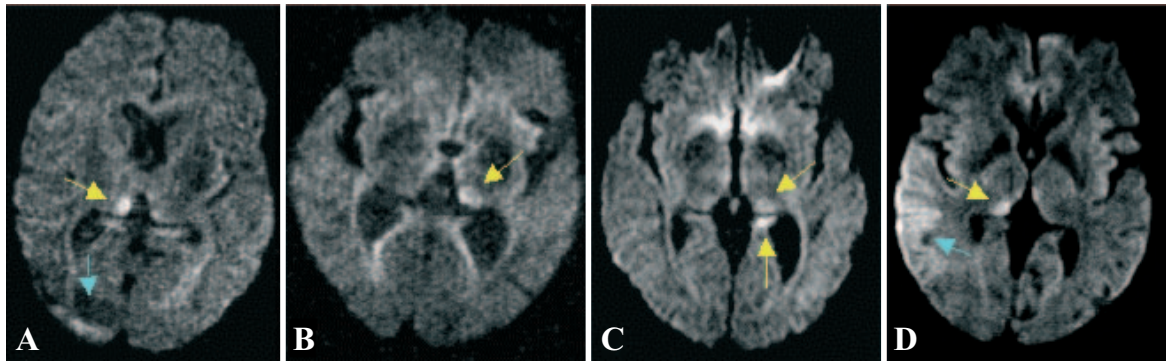


Fig. 2 Diffusion-weighted MRI depicting involvement of the pulvinar region of the thalamus in patients 2, 4, 6 and 10 (A–D) in almost identical areas across the five patients. Extratemporal cortical hyperintensity in patients 2 and 10 is also shown (A, D).

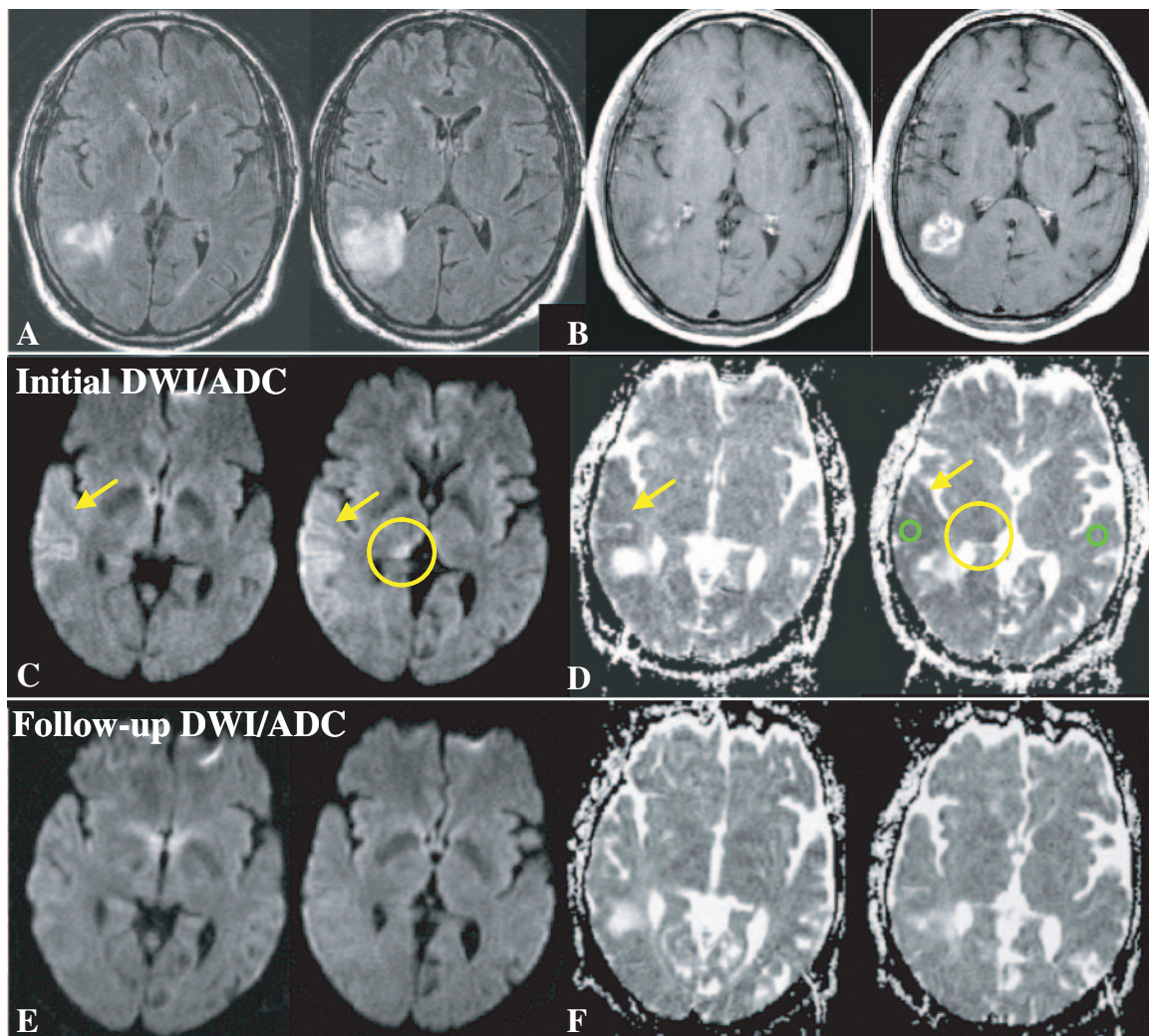


Fig. 3 Initial and follow-up MRI in patient 10. T2-weighted FLAIR images (A) and corresponding T1-weighted images after contrast injection (B) demonstrate enhancing lesion in the right temporoparietal region with central necrosis, which was confirmed as glioblastoma multiforme by histopathology. Acute diffusion-weighted MRI (C) and corresponding ADC (D) maps in the initial phase. Reduced diffusion and hyperintensity on the diffusion-weighted MRI is noted in the right posterior thalamus (yellow circle) and in temporal and parietal cortical regions (arrows). On the ADC maps, hyperintensity (increased diffusion) is noted in the contrast-enhancing centre of the glioblastoma, while there is surrounding hypointensity indicating extensive involvement of cortical structures due to epileptic activity (arrows; ROI for ADC assessment in green). Follow-up diffusion-weighted MRI (E) and ADC maps (F) demonstrate normalization of the areas with initially reduced diffusion while the neoplastic lesion is unchanged.

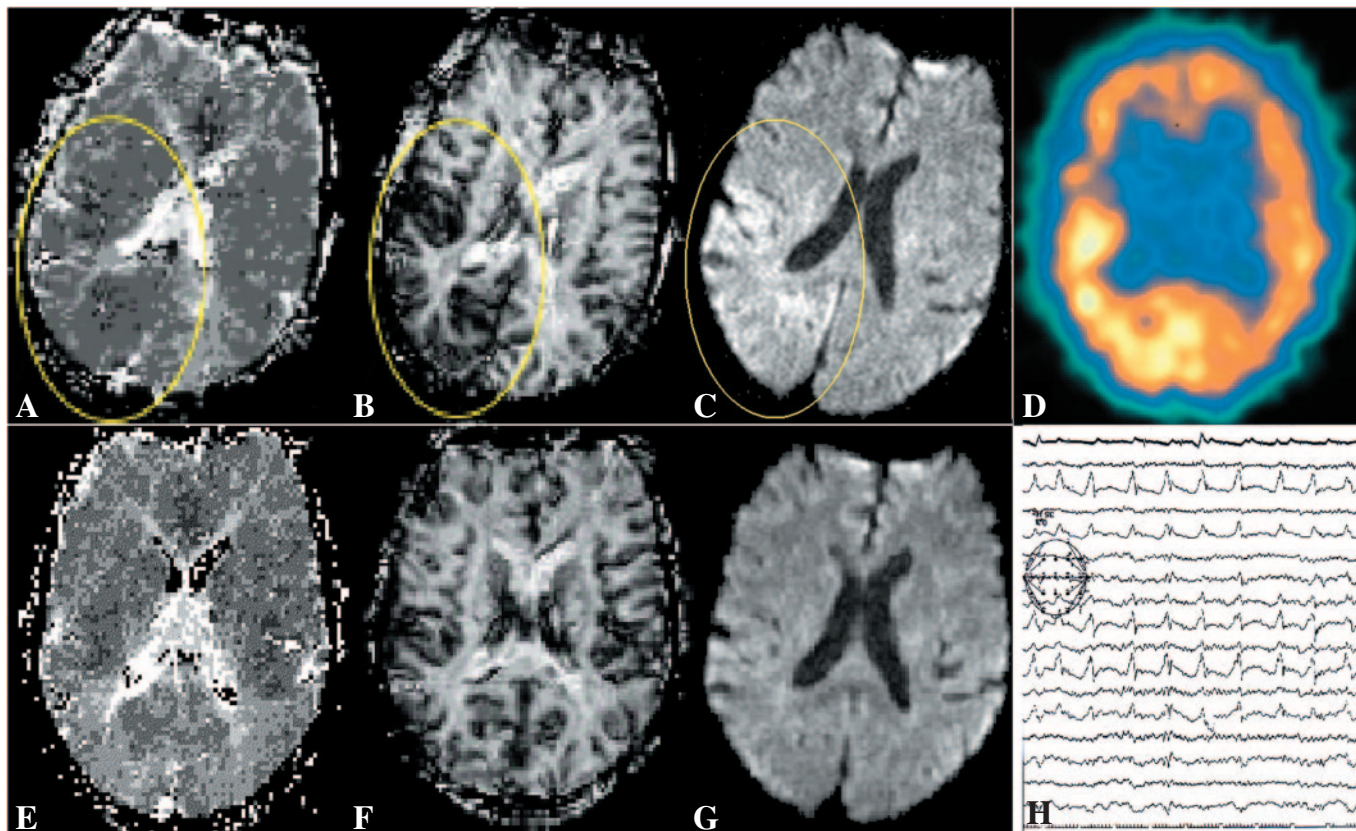


Fig. 4 Diffusion and perfusion MRI, follow-up MRI, initial SPECT study and EEG recording of patient one. Initial PI and DWI—time-to-peak (A), cerebral blood volume-(B) and diffusion-weighted image (C)—demonstrate hyperperfusion and hyperintensity on diffusion-weighted MRI in the right occipital and parietal cortex (encircled). This matches the area of hyperperfusion identified on SPECT (D). The follow-up MRI demonstrates normalisation of hyperperfusion and diffusion-weighted abnormality (E–G). EEG demonstrated PLEDs indicating ictal activity in the acute phase (H).

on day 2 or day 7. In patients 1, 2, 4, 7 and 9, DWI and ADC abnormalities resolved gradually and were normalized on follow-up examinations performed at day 14 or later. T2 signal change persisted over a longer period of time, but also completely resolved in those patients who were followed over a period of 2 weeks or longer: patients 1, 2, 4, 7 and 9 were followed over a period of 14 days to 10 months and showed complete lesion resolution.

Discussion

This study reports the combined use of DWI and PI in patients with CPSE. The findings demonstrate consistently the presence, location and extent of acute MRI changes in the ictal and peri-ictal phase of CPSE in patients with symptomatic epilepsy syndromes. In particular, acute DWI hyperintensity of the pulvinar is a new finding, adding to the increasing body of MRI data in patients with peri-ictal imaging changes. To us it was remarkable that, in a patient group that was quite heterogeneous in relation to the underlying causes of epilepsy, very similar patterns of acute MRI findings were present. There are several points that appear of particular interest in this regard.

There was a close spatial correlation of the location of DWI and PI changes, hyperperfusion on SPECT (in two patients) and the localization of regional EEG pathology, well demonstrated in patient 1 (Fig. 4). The combination of clinical symptoms, along with the time course of their resolution and EEG findings, indicates that the lesions detected by DWI and PI are consequences of prolonged focal epileptic activity and suggest pathophysiological links between ictal brain activity, haemodynamic changes and early parenchymal abnormalities. The finding of combined signs of hyperperfusion and reductions of the ADC in patients with focal status epilepticus is limited to few patients (Lansberg *et al.*, 1999) and there are no studies combining DWI and PI in the ictal phase. In a study with a similar methodology, drug-resistant epilepsy patients were examined in the interictal phase. The authors found an increased diffusion coefficient, which might possibly demonstrate the long-term course of acute phase findings (Heiniger *et al.*, 2002).

Reductions in brain water diffusion following the application of electroshock stimulation or ictal activity have been investigated in several experimental studies. Decreases in the ADC of the order of 9% were seen with short (0.1–10 s) trains of cortical electroshock stimulation (Zhong *et al.*, 1997).

A 17% reduction in ADC was seen with a longer stimulation duration with the proconvulsive gas flurothyl (28 min) (Zhong *et al.*, 1995). Prolonged ictal activity is known to increase glucose utilization, the increase of which is not adequately matched by the enhanced blood flow (Blennow *et al.*, 1979, 1985; Bruehl *et al.*, 1998). As a result, blood flow–metabolism uncoupling leads to a reduction of high-energy adenosine phosphates and tissue hypoxia, thereby stimulating anaerobic glycolysis. The duration of ictal activity may be the critical factor responsible for the changes which were detected by PI and DWI. It is conceivable that the observed regional hyperperfusion served as a compensatory mechanism yet was insufficient to prevent the stimulation of anaerobic glycolysis due to the prolonged ictal activity. As a consequence of compromised energy metabolism, ADC reductions may have developed. PI and DWI would therefore detect the consequences of ictal overactivation.

Using PI and DWI, we would not think that it is possible to locate the epileptogenic focus. However, it is likely that the tissue involved by seizure spread in the prolonged overactivation can be located with this method. Given the current limitations in regard to spatial and temporal resolution, it may indeed be very difficult for future MRI studies to differentiate the epileptogenic focus from areas of seizure spread.

We identified different areas of DWI changes: acute DWI hyperintensity in the hippocampal formation, the pulvinar region of the thalamus or DWI hyperintensity in mainly cortical areas adjacent to the primary pathology but clearly involving normal-appearing cortical tissue. The acute DWI hyperintensity involving the posterior part of thalamus, the nuclei pulvinare thalami, demonstrated in nine of our patients, is a novel MRI finding in epilepsy patients (Fig. 2). Several lines of evidence suggest that thalamic nuclei are involved in various epilepsy syndromes. In 1954 Penfield and Jasper suggested extensive interrelationships of the thalamic lateralis posterior pulvinar complex with the temporoparietal cortex (Penfield and Jasper, 1954). Postictal T2 hyperintensity was noted in the posterior thalamus on T2-weighted MRI in a patient with a right parietal seizure focus (Nagasaka *et al.*, 2002). This phenomenon on DWI in an acute peri-ictal state provides further evidence for a potential role of anatomical connections between the thalamus and mesial temporal lobe structures in symptomatic epilepsy and may add to the understanding of the extensive pulvinocortical relationships (Shipp, 2003).

For clinicians, isolated signal change restricted to the hippocampal area and/or the pulvinar may provide a diagnostic clue to the underlying pathology of prolonged confusional syndromes, especially in the elderly or in patients with other primary pathologies. Also, cortical and subcortical DWI changes not respecting vascular territories raise suspicion of a non-vascular mechanism (Lansberg *et al.*, 1999). Furthermore, the combination of hyperintensity on DWI with slight ADC alteration in the presence of signs of hyperperfusion in several arterial territories is a combination of MRI findings that is unlikely to be confused with territorial ischaemia. If

no other primary brain pathology is present, theoretically encephalitis might induce similar MRI changes, but to our knowledge no systematic studies on DWI and PI in encephalitis are available to date. The MRI protocol used in this study very much resembles the strategy employed in acute stroke studies. Of course, additional DWI and structural MRI sequences focusing on the hippocampus, thalamus and possibly the primary pathology should be added.

PI and DWI can provide information complementary to high-resolution structural MRI in the peri-ictal phase of status epilepticus. Integration of acute DWI and PI results with clinical and EEG results may be helpful to fully appreciate the role of acute tissue changes in postictal clinical syndromes. Combined PI and DWI provides information on the location and extent of early haemodynamic and tissue changes caused by ictal activity.

Acknowledgement

The authors wish to thank Dr Richard Wennberg from the Krembil Neuroscience Centre, University of Toronto, Canada, for his helpful comments on the manuscript.

References

- Blennow G, Folbergrova J, Nilsson B, Siesjo BK. Cerebral metabolic and circulatory changes in the rat during sustained seizures induced by DL-homocysteine. *Brain Res* 1979; 179: 129–46.
- Blennow G, Nilsson B, Siesjo BK. Influence of reduced oxygen availability on cerebral metabolic changes during bicuculline-induced seizures in rats. *J Cereb Blood Flow Metab* 1985; 5: 439–45.
- Bruehl C, Hagemann G, Witte OW. Uncoupling of blood flow and metabolism in focal epilepsy. *Epilepsia* 1998; 39: 1235–42.
- de Crespigny A, Rother J, van Bruggen N, Beaulieu C, Moseley ME. Magnetic resonance imaging assessment of cerebral hemodynamics during spreading depression in rats. *J Cereb Blood Flow Metab* 1998; 18: 1008–17.
- Detre JA, Sirven JI, Alsop DC, O'Connor MJ, French JA. Localization of subclinical ictal activity by functional magnetic resonance imaging: correlation with invasive monitoring. *Ann Neurol* 1995; 38: 618–24.
- Diehl B, Najm I, Ruggieri P, Foldvary N, Mohamed A, Tkach J. *et al.* Periictal diffusion-weighted imaging in a case of lesional epilepsy. *Epilepsia* 1999; 40: 1667–71.
- Fabene PF, Marzola P, Sbarbati A, Bentivoglio M. Magnetic resonance imaging of changes elicited by status epilepticus in the rat brain: diffusion-weighted and T2-weighted images, regional blood volume maps, and direct correlation with tissue and cell damage. *Neuroimage* 2003; 18: 375–89.
- Gass A, Gaa J, Sommer A, Hirsch J, Georgi M, Hennerici MG *et al.* [Echo-planar diffusion-weighted MRI in the diagnosis of acute ischemic stroke: characterisation of tissue abnormalities and limitations in the interpretation of imaging findings]. *Radiologe* 1999; 39: 695–702.
- Gyngell ML, Back T, Hoehn-Berlage M, Kohno K, Hossmann KA. Transient cell depolarization after permanent middle cerebral artery occlusion: an observation by diffusion-weighted MRI and localized 1H-MRS. *Magn Reson Med* 1994; 31: 337–41.
- Heiniger P, el-Koussy M, Schindler K, Lovblad KO, Kiefer C, Oswald H, *et al.* Diffusion and perfusion MRI for the localisation of epileptogenic foci in drug-resistant epilepsy. *Neuroradiology* 2002; 44: 475–80.
- Hufnagel A, Weber J, Marks S, Ludwig T, De Greiff A, Leonhardt G *et al.* Brain diffusion after single seizures. *Epilepsia* 2003; 44: 54–63.

- Jackson GD, Connelly A, Cross JH, Gordon I, Gadian DG. Functional magnetic resonance imaging of focal seizures. *Neurology* 1994; 44: 850–6.
- Kim JA, Chung JI, Yoon PH, Kim DI, Chung TS, Kim EJ et al. Transient MR signal changes in patients with generalized tonicoclonic seizure or status epilepticus: periictal diffusion-weighted imaging. *AJNR Am J Neuroradiol* 2001; 22: 1149–60.
- Lansberg MG, O'Brien MW, Norbash AM, Moseley ME, Morrell M, Albers GW. MRI abnormalities associated with partial status epilepticus. *Neurology* 1999; 52: 1021–7.
- Lee SH, Goldberg HI. Hypervascular pattern associated with idiopathic focal status epilepticus. *Radiology* 1977; 125: 159–63.
- Markand ON, Salanova V, Worth R, Park HM, Wellman HN. Comparative study of interictal PET and ictal SPECT in complex partial seizures. *Acta Neurol Scand* 1997; 95: 129–36.
- Nagasaka T, Shindo K, Hiraide M, Sugimoto T, Shiozawa Z. Ipsilateral thalamic MRI abnormality in an epilepsy patient. *Neurology* 2002; 58: 641–4.
- Ostergaard L, Weisskoff RM, Chesler DA, Gyldensted C, Rosen BR. High resolution measurement of cerebral blood flow using intravascular tracer bolus passages. Part I: Mathematical approach and statistical analysis. *Magn Reson Med* 1996; 36: 715–25.
- Penfield W. The evidence for a cerebral vascular mechanism in epilepsy. *Ann Intern Med* 1933; 7: 303–10.
- Penfield W, Jasper H. *Epilepsy and the functional anatomy of the human brain*. Boston: Little Brown; 1954.
- Shipp S. The functional logic of cortico-pulvinar connections. [Review]. *Philos Trans R Soc Lond B Biol Sci* 2003; 358: 1605–24.
- Shneker BF, Fountain NB. Assessment of acute morbidity and mortality in nonconvulsive status epilepticus. *Neurology* 2003; 61: 1066–73.
- Stone JL, Hughes JR, Barr A, Tan W, Russell E, Crowell RM. Neuroradiological and electroencephalographic features in a case of temporal lobe status epilepticus. *Neurosurgery* 1986; 18: 212–6.
- Warach S, Levin JM, Schomer DL, Holman BL, Edelman RR. Hyperperfusion of ictal seizure focus demonstrated by MR perfusion imaging. *AJNR Am J Neuroradiol* 1994; 15: 965–8.
- Wieshmann UC, Symms MR, Shorvon SD. Diffusion changes in status epilepticus. *Lancet* 1997; 350: 493–4.
- Yamada K, Wu O, Gonzalez RG, Bakker D, Ostergaard L, Copen WA et al. Magnetic resonance perfusion-weighted imaging of acute cerebral infarction: effect of the calculation methods and underlying vasculopathy. *Stroke* 2002; 33: 87–94.
- Zhong J, Petroff OA, Prichard JW, Gore JC. Barbiturate-reversible reduction of water diffusion coefficient in flurothyl-induced status epilepticus in rats. *Magn Reson Med* 1995; 33: 253–6.
- Zhong J, Petroff OA, Pleban LA, Gore JC, Prichard JW. Reversible, reproducible reduction of brain water apparent diffusion coefficient by cortical electroshocks. *Magn Reson Med* 1997; 37: 1–6.